WELDING RESEARCH

SUPPLEMENT TO THE WELDING JOURNAL, SEPTEMBER 1973

Sponsored by the American Welding Society and the Welding Research Council

Weld Cooling Rates and Heat-Affected Zone Hardness in a Carbon Steel

Study shows that hardness is related to cooling rate at a particular temperature and considers the implications for welding

BY B. A. GRAVILLE

ABSTRACT. Cooling rates have been widely used as a means of relating weld and heat-affected zone (HAZ) hardness to welding parameters. There is, however, no agreement on which temperature should be used for measuring cooling rates and in some instances difficulties have arisen because of the particular temperature chosen. Accordingly, experiments have been carried out to provide some experimental justification for the assumption that hardness can be related to cooling rate at some temperature and to determine that temperature for a carbon steel. Studies of cooling behavior and weld metal and heat affected zone hardness as a function of energy input and thickness have been made.

The results show that cooling behavior changes during transformation and in thick plate (3D cooling) this is equivalent to an increase in the thermal conductivity below about 450 C. Data is presented enabling cooling rates at a variety of temperatures to be determined for both thick and thin (3D and 2D) plate conditions. The results of hardness tests show that for a range of hardnesses (275-375 HV) the temperature of correlation is about 400-450 C but decreases to about 300 C when hardnesses of 400-425 HV are produced in the HAZ.

Introduction

The properties of welded joints and the possibility of cracking depends to a great extent on the cooling rate after welding. The concept of critical cooling rates has been used in attempts to predict safe welding procedures (i.e., preheat, energy input, etc., to avoid cold cracking) for carbon and low alloy steels. Cottrell (Ref.1) for example found a relation between the occurrence of cold cracking and the cooling rate at 300 C. Ito and Bessyo (Ref. 2) have related the occurrence of cracking in restrained butt welds to the cooling time between 300-100 C.

Recently, Bailey (Ref. 3) has presented a system for determining safe welding procedures based on a critical heat-affected zone (HAZ) hardness criterion. He used the cooling rate at 300 C to relate to the hardness. Bailey encountered certain difficulties with this approach when preheat was used. It became apparent that for some of his steels the hardness was determined by the cooling rate at a temperature higher than 300 C and it was necessary to apply a correction factor. Many other suggestions have been put forward for ways of characterizing the cooling cycle, (such as cooling time between 800-500 C, cooling rate at 540 C) so as to relate to the resulting hardness although there has been no experimental basis for any of these.

Cooling rates have been measured by a number of workers, and recently Signes (Ref. 4) has presented data covering a wide range of thicknesses, energy inputs and preheat levels. Most of these workers have found that cooling rate data fit the form of the theoretical equations quite well but with different values for the constants.

No work is known where the cooling rates over a range of temperatures were studied.

In the present work an attempt is made to provide some experimental justification to the assumption that hardness in the heat-affected zone and weld metal can be related to cooling rate and to determine at what temperature the cooling rate should be measured. The work also presented the opportunity of studying cooling rates at various temperatures and this has proved useful in correlating data in the literature and in explaining some of the anomalies.

Method of Approach

For a bead-on-plate test with a given energy input the cooling rate will increase as the thickness increases. Above a certain thickness, however, the cooling rate becomes independent of the thickness. This thickness can be termed the 'saturation thickness'. The saturation thickness will depend on the energy input and on the temperature at which the cooling rate is measured. For a high temperature the saturation thickness would be quite small whereas for a low temperature it would be greater.

In a similar manner the hardness (in the HAZ or the weld metal) will increase as the thickness increases (at least for those steels in which hardness varies with cooling rate. This includes C, C-Mn and low alloy steels). Again there will be a saturation thickness above which the hardness will not increase. In essence the program consists of measuring the saturation thickness for hardness and comparing it with the saturation thickness for cooling rates measured at different temperatures.

The program therefore falls into two parts: firstly, the study of cooling rates in welds over a range of thicknesses and energy inputs and secondly, the study of HAZ and weld metal hardnesses as a function of thickness and energy input. In this study no attempt was made to examine the effect of preheat.

B. A. GRAVILLE is Supervisor, Technical Research, Dominion Bridge Co., Ltd., Lachine, P.Q., Canada. *Paper was selected as alternate for the 54th AWS Annual Meeting in Chicago during April 2-6, 1973.*

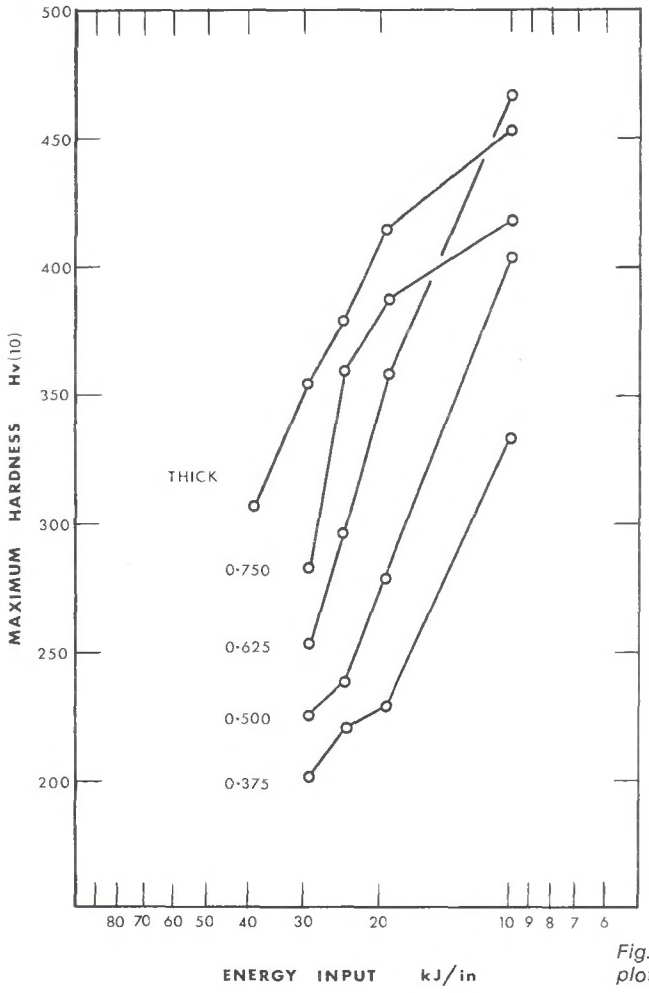

Fig. 1 — Maximum hardness of the HAZ of submerged arc welds plotted as a function of energy input for several thicknesses

Fig. 2 — The mean of the maximum HAZ hardness in thick plate as a function of energy input for SAW and SMAW deposits

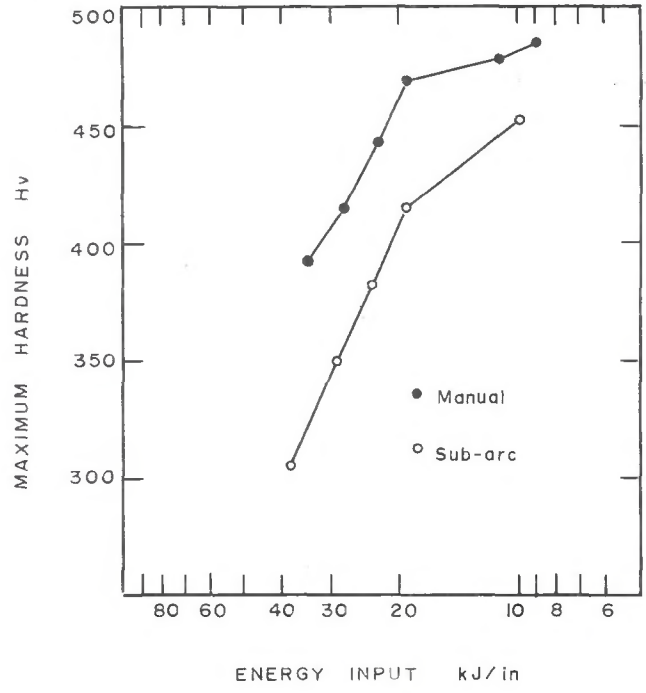

NOTATION

- T = Temperature
- T_o = Initial plate temperature
- K = Thermal conductivity
- C = Specific heat
- ρ = Density
- P = Thickness
- q = Rate of heat input
- E = Energy input
- H = Heat input ($H=\eta E$ where η is arc efficiency)
- P_s = Saturation thickness
- t = Time
- λ = $\rho^c/2K$
- V = Welding speed
- h = Coefficient of surface transfer
- r = $(X^2 + Y^2)^{1/2}$ — coordinates

Theoretical Background

The theoretical basis of heat flow in welding has been available for some time (Refs. 5,6) and has recently been summarized (Ref. 7). In thin plates, heat flow conditions are two dimensional (2D) and the cooling rate on the weld centerline is given by:

$$\left(\frac{dT}{dt}\right)_T = 2\pi K\rho C P^2 \frac{(T - T_o)^3}{H^2} \quad (1)$$

In thick plate conditions are three dimensional (3D) and the cooling rate is given by:

$$\left(\frac{dT}{dt}\right)_T = 2\pi K \frac{(T - T_o)^2}{H} \quad (2)$$

In plates of intermediate thickness the conditions are termed 2.5D and charts (Ref. 8) have been presented to describe this region. The saturation thickness (P_S) can be defined as the thickness at which equations (1) and (2) give the same cooling rate. Equating (1) and (2) gives:

$$P_S^2 = \frac{H}{\rho C (T - T_o)}$$

These equations assume that the physical properties (C, ρ, K) of the material do not change with temperature. In practice it is known that they are dependent on temperature and this makes it difficult to predict accurate values of cooling rate using these equations.

In general, too, at high energies and particularly in thin plates, there will be significant losses of heat by surface transfer.

Integration of equation (1) shows that the time t for the weld to cool to temperature T under 3D conditions is where A_{3D} is a constant dependent on the heat input, H, and the other constant depends on the choice of origin.

Likewise the time for a weld under 2.D conditions to cool to temperature T will be:

$$t = \frac{1}{A_{3D}}\left(\frac{1}{T - T_o}\right) + \text{Const} \quad (3)$$

$$t = \frac{1}{A_{2D}}\left(\frac{1}{T - T_o}\right)^2 + \text{Const} \quad (4)$$

In general a weld will start to cool under 3D conditions and change to 2D conditions at a lower temperature. Analyzing a cooling curve in the form of equations (3) and (4) thus provides a ready way of determining the mode of heat flow at any temperature.

Experimental

Cooling Rates

The cooling cycles of bead-on-plate welds using the submerged arc process were measured using Pt-Pt/13% Rh thermocouple. The plates were a minimum of 12 in. wide which allowed temperatures down to 100 C to be measured without edge effects. The thermocouple was manually inserted into the weld pool through the slag immediately behind the arc and the output of the thermocouple was recorded on a fast response strip chart recorder.

The loose flux and slag were not removed from the weld during the cooling period. Most of the heat used to melt the flux is conducted into the weld at high temperature because of the intimate contact between the metal and the slag and because of the insulating effect of the loose flux above the slag. The heat remaining in the slag when it detaches from the weld is small compared with the total heat input and thus the submerged arc process has a high efficiency (~95%).

Thicknesses from 0.24 in. to 4 in. and energy inputs from 4.4 to 126 kJ/in. were covered. The weld metal was a conventional silicon killed C/Mn weld metal giving an approximate chemistry of 0.1%C, 1.0%Mn, 0.3%Si.

Hardness Measurements

The steel chosen for the hardness measurements was ASTM A515 Grade 70 with a composition of 0.24C, 0.87Mn, 0.19Si. The steel was chosen because a wide range of HAZ hardnesses can be achieved over a relatively narrow range of cooling rates. The wide range of hardnesses is necessary because of the inherent inaccuracies in measuring hardness.

Beads were deposited in shallow grooves on the surface of a tapered plate. The plate was 36 in. by 36 in. and tapered from 3 in. thick at one end to 0.25 in. thick at the other. Five beads using the submerged arc process (dc electrode +ve) and five using E7018 manual electrodes (ac) were deposited. The energy inputs of the ten beads are shown in Table 1.

Sections were cut transverse to the beads at different thicknesses and hardness measurements were made in the HAZ and weld metal. At least five indentations close to the fusion boundary in the HAZ and two in the weld metal were made using a Vickers hardness machine with a 10 kg. load. The maximum value of the five was taken as the maximum HAZ hardness for that particular section.

Ten of the sections were at the thick end of the taper and the HAZ hardness in each bead was expected to be constant. These values were thus averaged to give a good estimate of the maximum HAZ hardness on thick plate for each bead. The values also provided a measure of the accuracy of measurement of hardness values. The results were plotted as HAZ hardness against energy input for each thickness. Some of the results are shown in Fig. 1 and complete results are listed in Tables 2, 3 and 4.

The mean of the maximum hardness values for the thick end are plotted in Fig. 2, for the submerged arc and the manual process. Higher hardnesses are achieved at the same energy input in the manual process because of its lower arc efficiency. To make the curves coincide a value of about 60% for the efficiency of the manual process relative to that of the submerged arc would have to be used. This low efficiency is in agreement with other work (Ref. 4) but might also be partly attributable to the use of ac for the manual tests where the power factor may have been low.

Table 1 — Conditions Used in the Hardness Test

Submerged arc welding:

Weld no.	Amp	Arc voltage	Speed, ipm	Energy, kJ/in.
S1	300	26	48.6	9.7
S2	300	26	24.3	19.3
S3	300	26	19.5	24.0
S4[a]	500	27	21.0	38.6
S5	400	27	22.4	29.0

Shielded metal-arc welding (E7018 electrodes):

Weld no.	Amp	Voltage	Speed, ipm	Electrode size, in.	Energy, kJ/in.
M1 (dc)	79	19	10	3/32	8.8
M1 (ac)[b]	90	21	10	3/32	11.3
M2 (ac)	116	22	8	1/8	19.2
M3 (ac)	112	22	6.5	5/32	22.8
M4 (ac)	166	22	8	5/32	27.4
M5 (ac)	166	22	6.5		34.0

(a) S4 weld was restricted to the thick end to avoid tempering of adjacent beads.
(b) M1 (ac) was a short run at the thick end of M1. The plate was allowed to cool completely between runs.

Results

Cooling Rates

The time and temperature data from the cooling curves was analyzed in a computer in the following way. Following equations 3 and 4, the curves $1/(T-T_o)$ versus t and $1/(T-T_o)^2$ versus t were generated. The slopes of these curves (A_{3D} and A_{2D}) were then determined as a function of temperature. The results were plotted out graphically by the computer and this enabled the heat flow mode to be determined at any temperature.

A typical cooling curve for thick plate (4 in.) in which 3D conditions obtain almost over the entire temperature range is shown in Fig. 3, plotted in the form $1/(T-T_o)$ versus t. To a good approximation, the curve can be considered as being composed of two lines with a fairly rapid change of slope at a temperature of about 450 C. This behavior was not observed in an austenitic weld metal and is therefore assumed to be associated with the transformation of the steel.

The slopes of the curves $1/(T-T_o)$ versus t at different temperatures for thick plate are plotted for five different energy inputs in Fig. 4. The change in cooling behavior for the lowest energy inputs is sharper and occurs at a slightly lower temperature than for the high energy inputs. This is consistent with the idea that the change results from the transformation since the start of transformation decreases with increasing cooling rate. The temperature at which the change in behavior occurs would be expected to depend on the composition of the weld metal.

From equation 1 for 3D conditions, the slopes (A_{3D}) of the graphs $1/(T-T_o)$ versus t would be expected to depend on the energy input E in the form $A_{3D} = B_{3D}/E$ where B_{3D} is a constant and the arc efficiency is assumed constant. Such a plot is shown in Fig. 5 for results at 700 C where a large number of the tests were in the 3D region. Good lines were obtained for other temperatures although as noted above the cooling behavior started to change at a lower temperature for the lower energy inputs. For practical purposes, however, the difference was small, and lines could be drawn through all the data at each temperature. The resulting values of B_{3D} are plotted against temperature in Fig. 6.

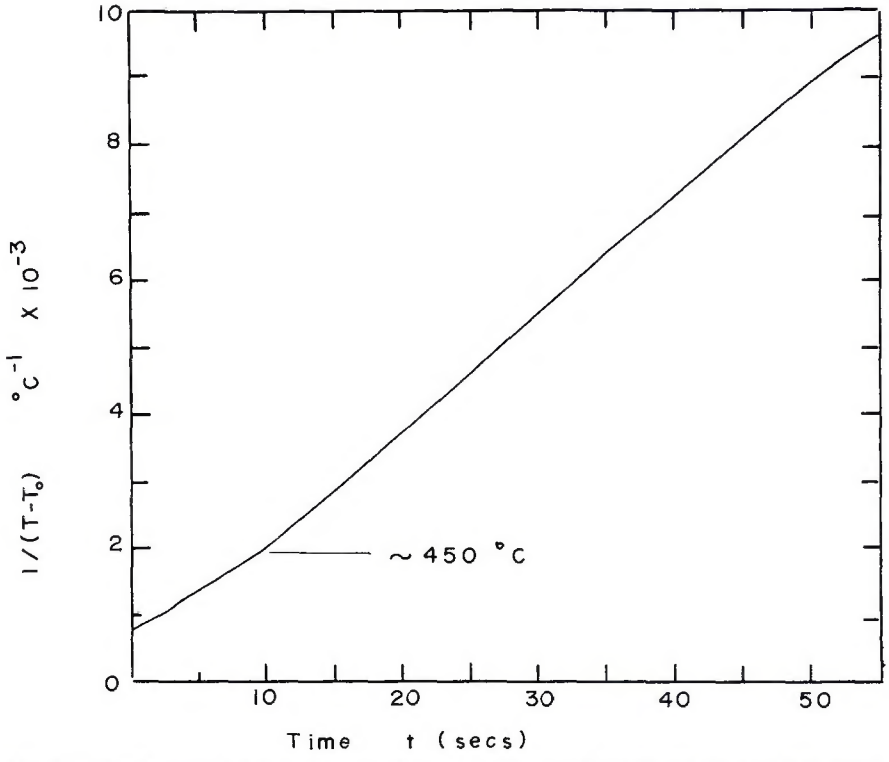

Fig. 3 — Cooling curve for a submerged arc weld (Energy input 29.4 kJ/in.) on 4 in. thick plate plotted in the form 1/(T-To) versus t. 3D conditions prevail almost over the entire range

Fig. 4 — Slopes A_{3D} of the curves 1/(T-To) versus t plotted as a function of temperature for five submerged arc deposits on 4 in. thick plate

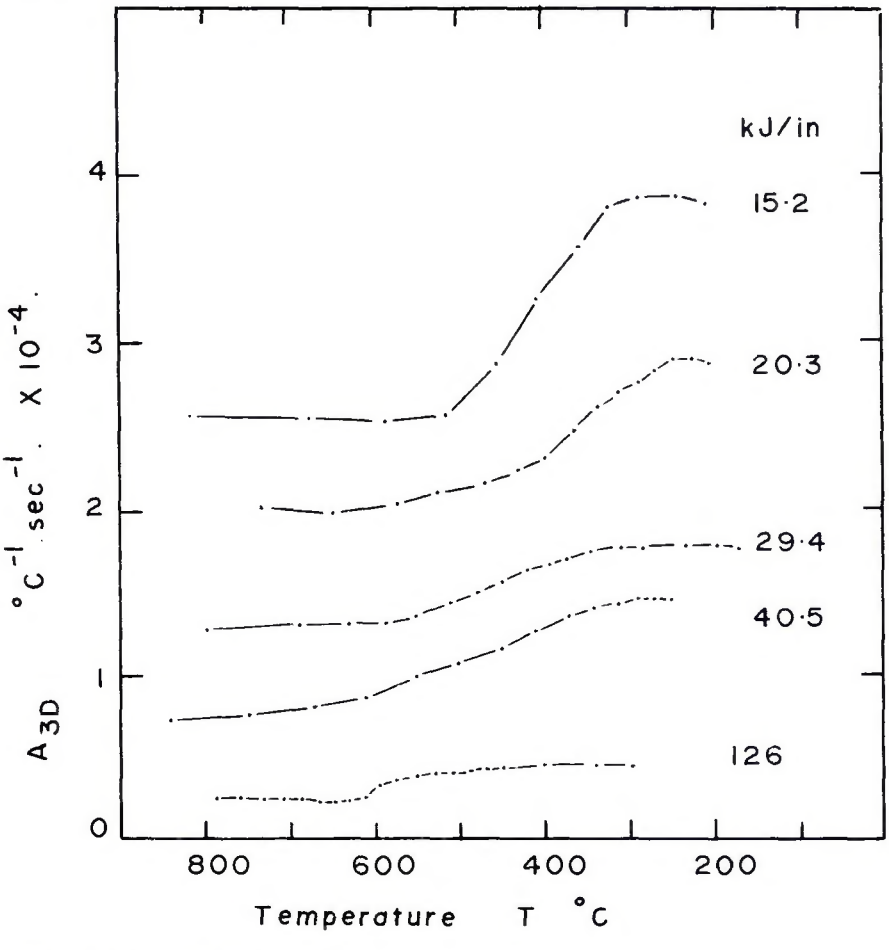

This enables the cooling rate at any temperature to be determined from the equation

$$\frac{dT}{dt} = B_{3D} \frac{(T - T_o)^2}{E} \qquad (5)$$

for 3D conditions for submerged arc welding. These values compare quite well with those of Signes.

Data for 2D conditions were analyzed in essentially the same way except that all data were corrected for surface transfer losses according to the method in the appendix. Following equation 4 the slopes A_{2D} of the plots $1/(T-T_o)^2$ versus t were plotted against P^2/E^2. This is shown in Fig. 7 for a temperature of 200 C where a large number of tests were in the 2D region. The slope of these curves (divided by 2 which comes from the differentiation) are plotted as a function of temperature in Fig. 8. These values enable the cooling rate to be determined from the equation

$$\frac{dT}{dt} = B_{2D} \frac{P^2}{E^2} (T - T_o)^3 \qquad (6)$$

for 2D conditions.

These values agree well with other published data. Equations 5 and 6 enable the saturation thickness P_S to be determined as a function of energy input at each temperature. Equating 5 and 6 leads to the relation:

$$P_s^2 = \frac{B_{3D}}{B_{2D}} \frac{E}{(T-T_o)}$$

where B_{3D} and B_{2D} are taken from Figs. 6 and 8 respectively. This relation provides the lines drawn in Figs. 10 and 11 for several temperatures. The saturation thickness may be useful for determining cooling rates in the 2 and 2.5D region where greater accuracy may be required. For a given energy the saturation thickness may be determined from Figs. 10 or 11. For a given plate thickness P the term $(P/P_s)^2$ becomes equivalent to Adam's relative thickness term and can be used directly (in Fig. 1 of Ref. 8) to calculate cooling rates in the 2 and 2.5D region.

It was interesting to note from the results that transition from 3D behavior to 2D occurred quite sharply — generally in a range less than 100 C. Within the limits of experimental error in these tests all of the data could be treated as either 3D or 2D (with surface transfer correction), and the use of solutions for the 2.5D region was not warranted.

Analysis of Hardness Data

In the thin end of the taper, where the hardness depends on thickness,

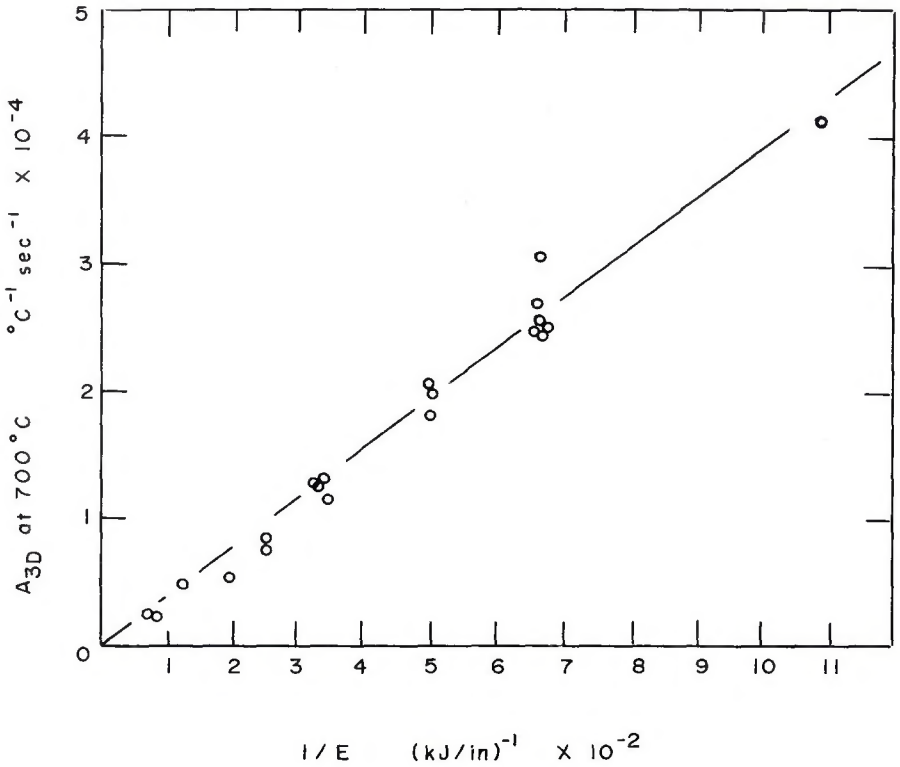

Fig. 5 — Parameter A_{3D} at 700 C plotted as a function of energy input

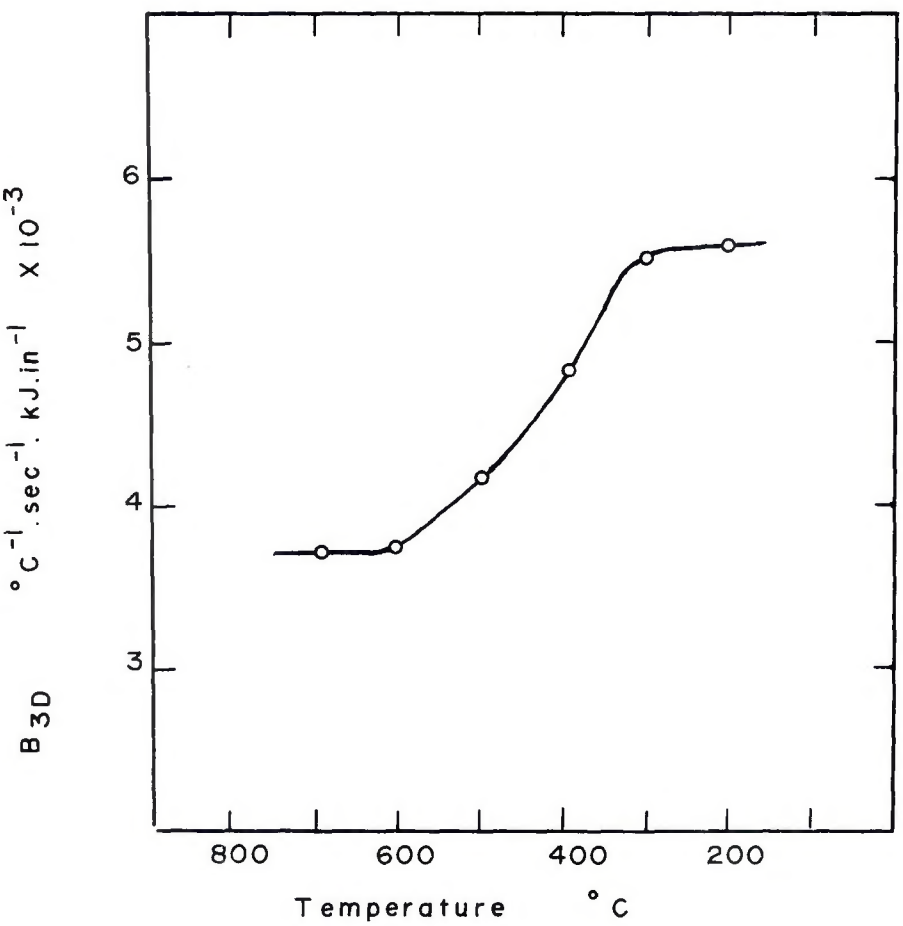

Fig. 6 — Parameter B_{3D} plotted as a function of temperature

2D heat flow conditions exist at the temperature of interest. The cooling rate is thus given by:

$$\frac{dT}{dt} = B_{2D} \frac{P^2}{E^2} (T - T_o)^3$$

If the hardness can be uniquely related to cooling rate at a particular temperature then constant hardness would imply constant cooling rate. Thus at constant hardness P^2/E^2 is constant or P is proportional to E.

Drawing a horizontal line through Fig. 1 at constant hardness provides values of P and E. These are plotted in Fig. 9 for one particular hardness. A good straight line relationship results and indicates that hardness can be uniquely related to cooling rate at some temperature. Good lines were obtained in all cases (with correlation coefficient greater than 0.95 in most cases). The line should go through the origin but there is a small positive intercept. A similar value of intercept was found on all such plots but the physical significance of this is not known.

At larger thicknesses the hardness becomes independent of the thickness and depends only on the energy input. This value is known quite accurately since the mean of ten values in the thick region are taken. The intersection of the lines gives the saturation point and the saturation thickness for hardness for the particular energy.

The results for several hardness levels in the HAZ are plotted in Fig. 10.

Comparison with the cooling rate data indicates that for the range of hardnesses 275 – 375 HV the hardness can be uniquely related to the cooling rate when measured at a temperature at about 400 – 450 C. For higher hardnesses (400 and 425 HV) a lower temperature of correlation is required. This corresponds to a decrease in the start of transformation, when substantial amounts of martensite are formed. The two points of 400 and 425 HV are confirmed by the results of the manual tests when account is taken of the difference in arc efficiency. A similar analysis was applied to the weld metal hardness results, and are shown in Fig. 11. These indicate a slightly higher temperature of correlation which would be expected from the lower carbon content. No hardnesses over 350 HV were obtained in the weld metal.

General Discussion

It is apparent from the graphs that the theoretical form of the cooling rate equations may be used to predict cooling rate if the appropriate values of the constants are chosen. The data

may also be useful in converting cooling rates at one temperature to those at another. The data contained in Fig. 6 are useful in explaining some of the anomalies in the literature. For example, Bradstreet (Ref. 9) presents data for cooling rates at 540 C which correspond to a value of B_{3D} equal to 5.2 $\times 10^{-3}$ kJ/in./sec/C deg. This value is closer to the values at 300 C in the present work. If the composition of this weld metal was such that transformation was occurring at higher temperatures, then the value of B_{3D} would be obtained at higher temperatures.

The variation of B_{2D} with temperature is not the same as B_{3D} although there is an increase through the transformation. The decrease at lower temperatures may have resulted from errors introduced by the surface transfer correction or may result from the decreasing specific heat of the steel.

The good correlation obtained in the constant hardness plots (Fig. 9) provides justification for using cooling rate measured at a temperature for relating to hardness. It is possible that an equally good correlation may have been obtained by using the time to cool over a certain range of temperatures such as 800-500 C. The effect of using a temperature range would be to 'round off' the transition between the 2D and 3D parts in Fig. 9. If the temperature range were large then there would be a gradual curve in Fig. 9 as it approaches thick conditions. From the plots of the types shown in Fig. 9, it can be inferred that in order to account for the relatively sharp transition observed, good correlation would only be achieved if the temperature range were less than about 300 C. Furthermore, misleading results would be obtained if the temperature range overlapped the start of the transformation.

Figure 10, showing the temperature of correlation, indicates that for a wide range of hardness (275 - 375 HV) the points lie close to a single temperature between 400-450 C. Likewise, all the points for the weld metal results lie between 400-500 C. The points for HAZ hardnesses of 400-425 HV (both from submerged arc welds and manual welds) lie close to 300 C. It is interesting to speculate that Cottrell found good correlation between cracking and cooling rate at 300 C because cracking was occurring when hardnesses of 400 HV and greater were formed. Certainly the recent evidence of Bailey suggests that under similar conditions a hardness of 400 HV or more would be required for cracking.

The fact that the temperature of correlation falls within the transformation range where cooling behavior is changing presents some problems in recommending temperatures for measuring cooling rates. Since the transformation range would be composition dependent, different cooling rates would be obtained for different steels for the same welding conditions. Since the object of specifying cooling rates would be to characterize the welding conditions irrespective of steel composition (at least over a limited range) either the cooling rate would have to be measured above the transformation or, if quoted at lower temperatures, use values of B_{3D}, B_{2D} from higher temperatures where they

Table 2 — Hardness Results,[a] HAZ of SAW Welds Made with Various Energy Inputs

Thickness	Energy input, kJ/in.				
in.	9.7	19.3	24.0	29.0	38.6
3.125	498	464	405	370	299
2.938	464	405	394	306	302
2.688	446	394	397	299	304
2.313	455	387	373	345	322
1.938	455	401	360	339	309
1.500	429	425	376	390	
1.375	450	387	401	336	
1.250	446	446	397	387	
1.125	459	450	373	345	
1.000	429	397	351	387	
	453[b]	416[b]	383[b]	350[b]	307[b]
0.875	455	383	373	348	
0.750	417	387	360	283	
0.727	442	390	354	299	
0.662	478	376	317	281	
0.625	468	357	297	254	
0.601	455	345	302	266	
0.528	514	302	276	249	
0.500	405	281	238	225	
0.450	433	287	272	232	
0.402	401	236	242	228	
0.375	333	230	221	201	
0.328	304	224	221	209	
0.287	287	236	227	232	

(a) The figures are the Vickers hardness numbers with 10 kgm load. Each figure is the maximum of five readings taken in the HAZ close to the fusion boundary.
(b) Mean value of the figures listed above, i.e., the figures for "thick" sections.

Table 3 — Hardness Results,[a] Weld Metal of SAW Welds Made with Various Energy Inputs

Thickness,	Energy input, kJ/in.				
in.	9.7	19.3	24.0	29.0	38.6
3.125	342	285	276	253	254
2.938	348	264	260	251	247
2.688	348	270	268	247	242
2.313	333	279	253	238	230
1.938	387	258	253	243	227
1.500	345	279	238	262	
1.375	361	270	245	240	
1.250	363	285	272	266	
1.125	380	285	245	243	
1.000	366	283	230	236	
	355[b]	276[b]	254[b]	248[b]	240[b]
0.875	339	258	245	245	
0.750	345	258	225	225	
0.727	294	262	242	233	
0.662	366	264	238	219	
0.625	363	247	201	209	
0.601	383	268	249	238	
0.528	231	258	228	215	
0.500	342	225	212	187	
0.450	327	236	235	213	
0.402	302	216	212	194	
0.375	276	206	201	193	
0.328	270	205	196	188	
0.287	242	201	202	215	

(a) The figures are Vickers Hardness numbers with 10 kgm load. Each figure is the higher of two readings in the weld metal.
(b) Mean value of the figures listed above, i.e., the figures for "thick sections."

are not influenced by the transformation.

One possible approach would be to standardize on one temperature (say 540 C) which is close to, but above, the start of transformation for many carbon manganese and low alloy steels. For thicknesses that would involve 2D heat flow the effective cooling rate would be determined using Adams' graphs but using the term $(P/P_s)^2$ for relative thickness where P_s is taken from the hardness data in Figs. 10 or 11, rather than the cooling rate data. In this way correct welding procedures can be determined on a critical hardness criterion. Although theoretically not very elegant, this approach is simple and appears to work quite well in practice.

Conclusions

The results of a study of weld cooling rates and heat-affected zone and weld metal hardnesses have led to the following conclusions.

1. The cooling behavior changes abruptly as the weld metal transforms. The change is equivalent to an increase in the thermal conductivity of the steel for 3D heat flow conditions.
2. The form of the theoretical equations may be used with the constants determined experimentally.
3. Heat-affected zone and weld metal hardness can be uniquely related to weld cooling rate at a temperature. The temperature depends on the level of hardness but is approximately constant for a wide range of hardnesses.

Acknowledgements

The author would like to thank Mr. L. Bigras and Mr. G. Montpetit for help with the experimental work, NRC (Canada) for financial assistance and Dominion Bridge Company Limited for permission to publish.

Appendix

Correction for surface transfer

At the lower temperatures particularly on the thinner material significant heat losses occur by surface transfer. Since the data was being analyzed in terms of conduction, it was necessary to correct some of the low temperature data. This was only done for the 2D analysis since solutions were readily available for this case (Ref. 5). The temperature distribution around a moving arc for the 2D mode where surface transfer heat losses are occurring is:

$$K_o(\delta) \rightarrow \exp(-\delta)\left(\frac{\pi}{2\delta}\right)^{1/2}$$

Table 4 — Hardness Results,[a] HAZ of SMAW Welds Made with Various Energy Inputs

Thickness in.	Energy input, KJ/in. 8.8 (dc)	19.2 (ac)	22.8 (ac)	27.4 (ac)	34.0 (ac)
3.125	—	493	478	429	429
2.938	498[b]	468	401	413	409
2.688	455[b]	503	508	413	380
2.313	514	464	455	397	383
1.938	473	478	446	397	397
1.500	483	437	405		360
1.375	503	503	442	421	455
1.250	488	473	442	394	380
1.125	514	429	437	473	370
1.000	483	442	429	383	373
	486[c]	469[c]	444 [c]	415[c]	394[c]
0.875	437	464	405	437	421
0.750	478	413	421	401	333
0.728	493	417	405	380	325
0.679	498	455	442	373	345
0.625	483	351	319	327	283
0.577	508	473	442	333	299
0.550	498	459	360	299	276
0.500	437	376	333	254	245
0.486	548	463	363	294	253
0.426	464	376	274	258	245
0.375	387	281	236	228	224
0.351	409	281	251	232	230
0.287	302	268	238	232	233

(a) Each figure is the maximum of five readings in the HAZ close to the fusion boundary.
(b) These were welded with ac energy, 11.3 kJ/in.
(c) Mean value of the figures listed above, i.e., the figures for "thick sections."

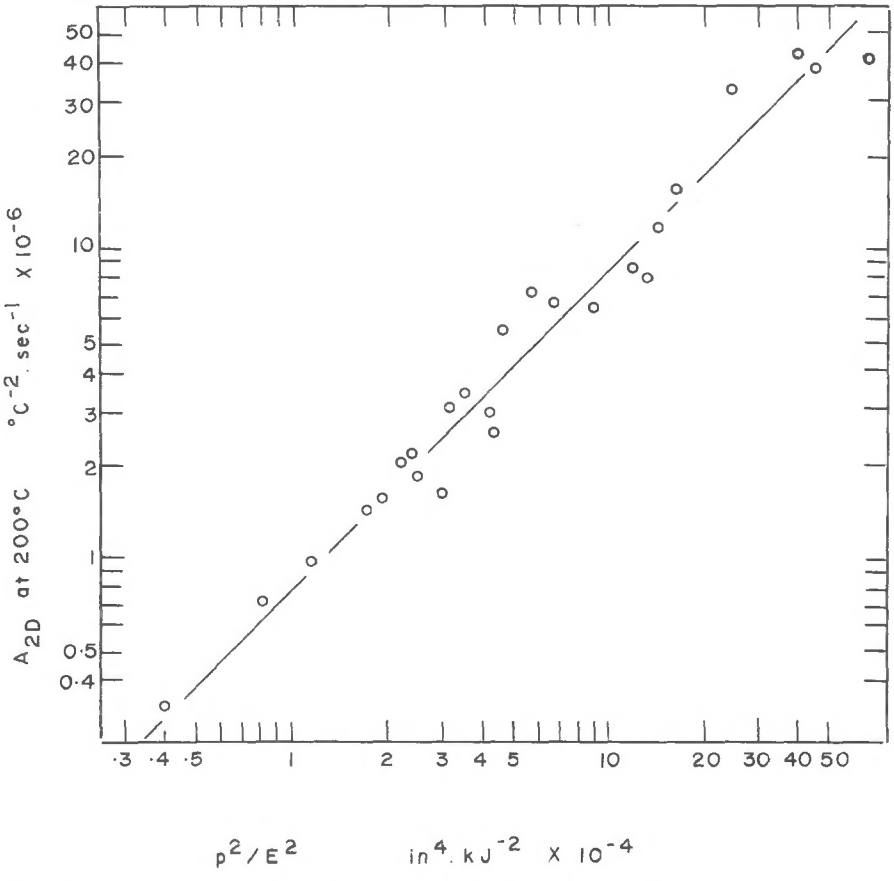

Fig. 7 — Parameter A_{2D} at 200 C plotted as a function of thickness, and energy input

Fig. 8 — Parameter B_{2D} plotted as a function of temperature

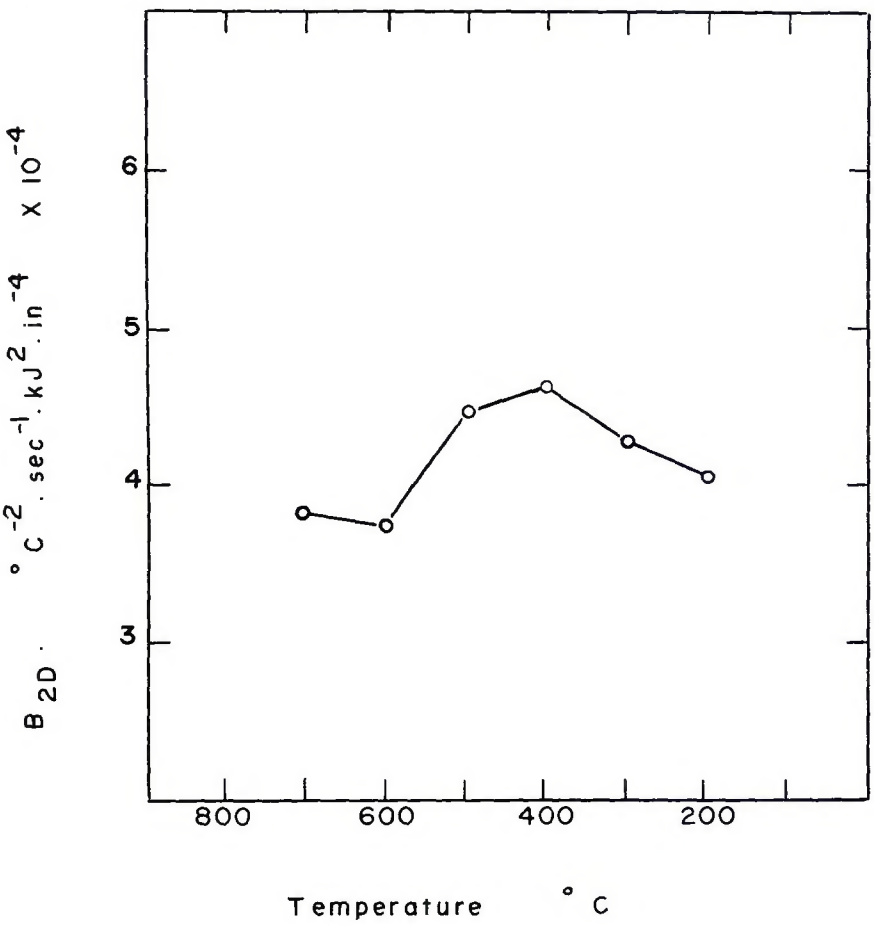

$$T_{(x,y)} = \frac{q}{2\pi KP} \exp(\lambda V_x) K_o \left\{ r \left(\lambda^2 V^2 + \frac{2h}{KP} \right)^{1/2} \right\}$$

For large values of the argument δ the Bessel function $K_o(\delta)$ can be approximated.

$$K_o(\delta) \rightarrow \exp(-\delta) \left(\frac{\pi}{2\delta} \right)^{1/2}$$

Making this approximation and assuming $\lambda^2 V^2 >> 2h/KP$ and, considering the weld centerline where $y = 0$ and $x = r$, we have

$$T_{(x,y)} = \frac{q}{2\pi KP} \exp \left(\frac{-rh}{\lambda V KP} \right) \left(\frac{\pi}{2r\lambda v} \right)^{1/2}$$

or

$$T_{st} = T_{2D} \exp \left(-\frac{rh}{\lambda V KP} \right)$$

where T_{2D} is the temperature that would have resulted if there had been no surface losses.

The equation can be further modified by eliminating the term r which in general is not known. This gives:

$$T_{2D} = T_{sT} \exp \left\{ \frac{h}{2\pi KP} \left(\frac{q}{C_p V T_{2D} P} \right)^2 \right\}$$

Thus the temperature T_{2D} that would have resulted in the absence of surface losses may be found from the real temperature T_{ST} from the above equation. This was done by iteration and by assuming reasonable values for the other terms. For h, a value of 0.0004 cal/sec/cm²/C deg was used having been determined in a separate experiment.

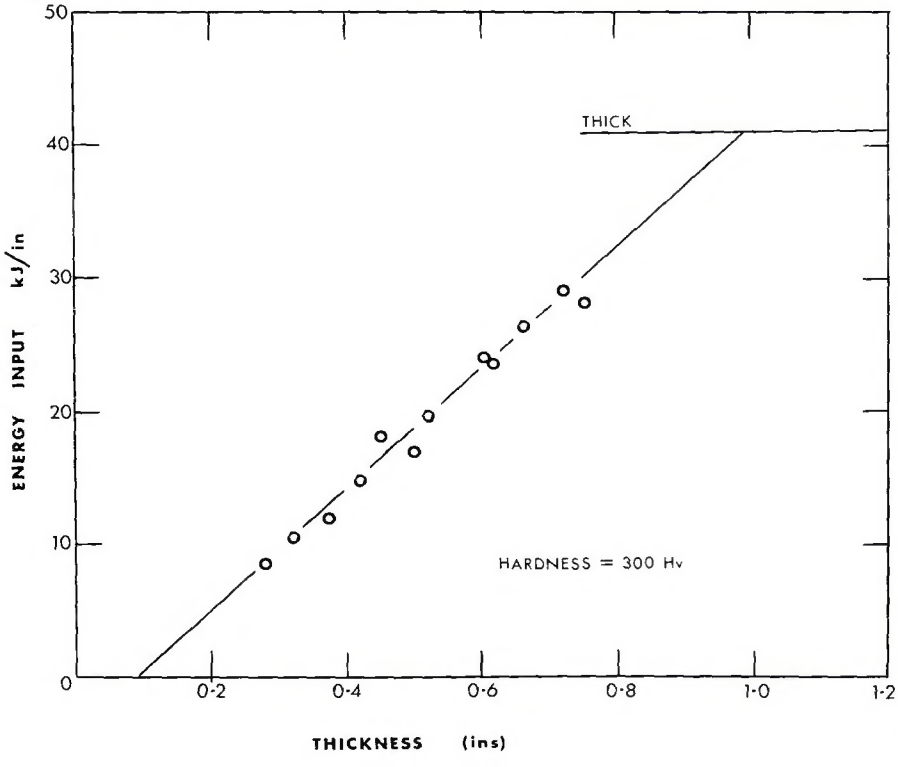

Fig. 9 — Plot of energy input against thickness for constant hardness of 300 HV. Results from the HAZ of submerged arc deposits. The line marked "Thick" is the energy input giving a hardness of 300 HV on thick plate and is the mean of ten values. The intersection of the lines represents the saturation point and gives the saturation thickness for the corresponding energy

References

1. Cottrell, C. L. M., Jackson, D. M., Whitman, J. G., Welding Research, 1951, *5*, (4), 201r.

2. Ito, Y., and Bessyo, K., "A prediction of welding procedure to avoid heat af-

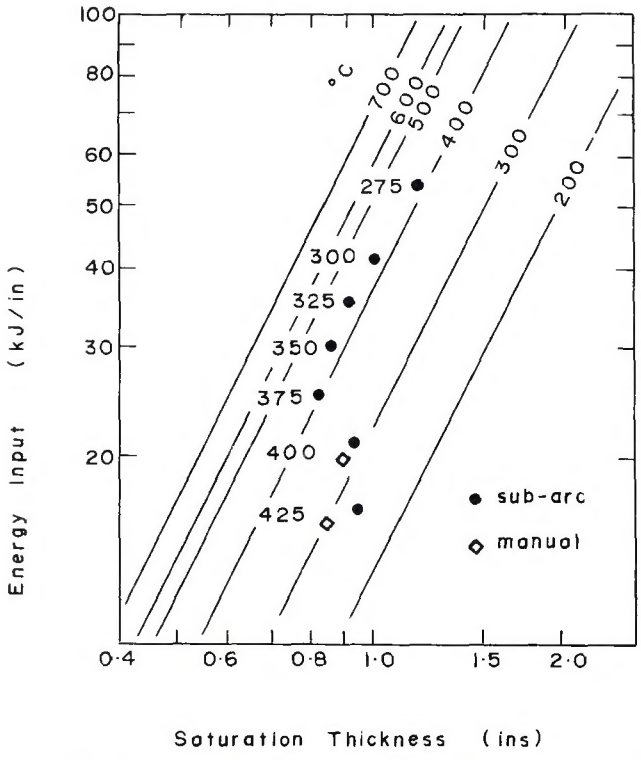

Fig. 10 — Energy input as a function of saturation thickness. The lines are derived from the cooling rate data and the points from hardness data. Results are for the HAZ of SAW and SMAW deposits

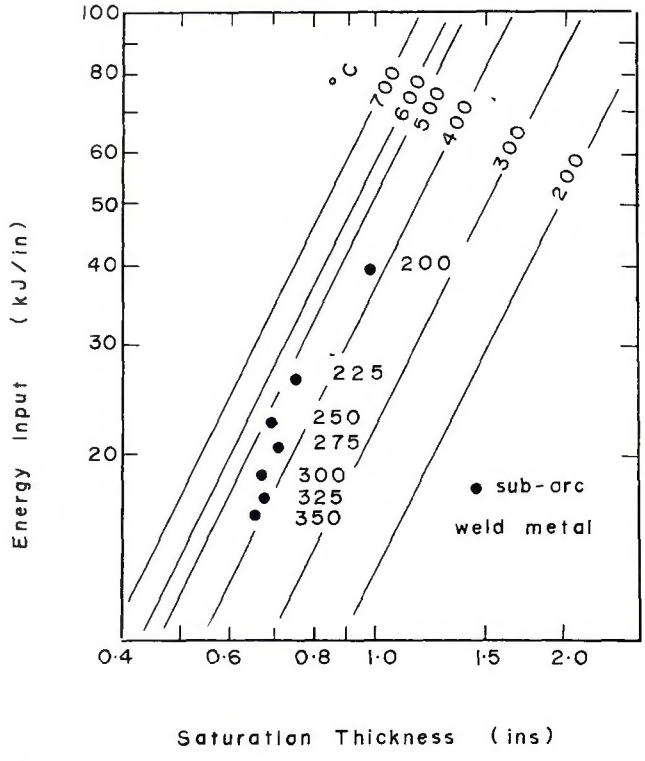

Fig. 11 — Similar plot to Fig. 10 for results from submerged arc weld metal

tected zone cracking," IIW Document No. IX-631-69.

3. Bailey, N., "Welding Procedures for low alloy steels," Welding Institute, July 1970.

4. Signes, E., "A Simplified Method of Calculating Cooling Rates in Mild and Low Alloy Steel Weld Metals," *Welding Journal,* 51, (10) Research Suppl., 473-s to 484-s, 1972.

5. Carslaw, M. S., and Jaeger, J. C., *Conduction of heat in solids,* Second edition, Oxford Press, London, U.K. (1959).

6. Rosenthal, D., ASME Trans., 849-866 (November) 1946.

7. Myers, P. S., Uyehara, O. A., and Borman, G. L., Welding Research Council Bulletin, No. 123, (July) 1967.

8. Jhaveri, P., Moffatt, W. G., and Adams, C. M., *Welding Journal,* Vol. 41, (1) Research Suppl., 12-s to 16-s (1962).

9. Bradstreet, B. J., *Welding Journal,* Vol. 34, (11) Research Suppl., 499-s to 504-s (1969).

WRC Bulletin
No. 179
Dec. 1972

Stress Indices and Flexibility Factors for Moment Loadings on Elbows and Curved Pipe

by W. G. Dodge and S. E. Moore

Flexibility factors and stress indices for elbows and curved pipe loaded with an arbitrary combination of in-plane, out-of-plane and torsional bending moments are developed for use with the simplified analyses procedures of present-day design codes and standards. An existing analytical method was modified for use in calculating these factors, the equations were programmed for the IBM-360 computer and computed results were compared with experimental data to establish the adequacy of the modified method. Parametric studies were then performed to obtain desired information. The results are presented in both tabular and graphical form. Approximate equations of best fit, developed from the tabulated values, are presented in a form which can be used directly in the codes and standards. The present equations are slightly more conservative than the ones in current use. However, experimental and analytical studies now in progress may indicate further modifications in the stress indices and flexibility factors for elbows.

The research presented in this paper was sponsored by the U.S. Atomic Energy Commission under contract with the Union Carbide Corporation. Publication was sponsored by the Pressure Vessel Research Committee of the Welding Research Council.

The price of *WRC Bulletin 179* is $3.50 per copy. Orders should be sent to the Welding Research Council, 345 East 47th Street, New York, N.Y. 10017.